Journal of Thermal Analysis, Vol. 35 (1989) 743–750

ISOTHERMAL AND NONISOTHERMAL GRAVIMETRY OF NONTRONITE DEHYDROXYLATION

N. S. Felix and *B. S. Girgis*

CMRDI, AND NATIONAL RESEARCH CENTRE, DOKKI, CAIRO, EGYPT

(Received August 24, 1987; in revised form October 31, 1988)

A pure typical nontronite from Czechoslovakia (Sampor) was analysed by the title techniques in the range 570–1070 K. The isothermal dehydroxylation of nontronite, recorded at 630–730 K, was described reasonably, in the decomposition range $\alpha = 0.05$–0.95, by diffusion-controlled mechanisms D_3 and D_4. Application of the current solid-state reaction equations to the non-isothermal curve gave very poor results, except in the limited decomposition range $\alpha = 0.10$ to 0.55. A unimolecular mechanism equation (F_1) and also a second-order (SO) mechanism gave the best linearization of the curve. The activation energies estimated from the isothermal (D_3, D_4) and non-isothermal (F_1) experiments were 125 and 151 kJ·mol^{-1}, respectively. Reduced time plots indicate the probable presence of a sequence of different mechanism for both techniques.

The structural and crystallochemical changes of clays during dehydration and dehydroxylation have been the subject of numerous investigations [1–11]. Thermogravimetry has indicated the increasing thermal stability of the OH groups in the structure of dioctahedral clay minerals in the sequence nontronite < fire-clay < kaolinite < montmorillonites. The kinetics of dehydroxylation of dioctahedral smectites has been shown to be affected by both the nature of the interlayer cation and the tetrahedral charge. Analysis of the TG curves of montmorillonites and nontronites indicated that the rate equation for three-dimensional diffusion in a spherical particle (D_3) is valid [11]. The previous results also proved that the Fe atoms in the octahedra have the greatest influence on the initiation of the dehydroxylation process, as in the Fe-rich mineral nontronite.

The present study presents a mathematical analysis of both dynamic and isothermal weight change experiments for a typical nontronite from Czechoslovakia. It aims at determination of the kinetic equations governing the process of dehydroxylation, as well as the associated activation energy under these conditions.

John Wiley & Sons, Limited, Chichester
Akadémiai Kiadó, Budapest

Experimental

A finely powdered nontronite deposit from Czechoslovakia (Sampor) was purified by dispersion in distilled water, decantation and redispersion, so as to remove the contaminating mineral deposits. The surface-floating material was finally decanted, filtered and dried at 380 K. Analysis by X-ray and electron microscopy proved that the solid was free from other minerals. Chemical analysis of the dry material gave the structural formula $(Si_{6.93}Al_{1.07})\ (Al_{0.06}Fe_{3.92}Ti_{0.02})O_{20}(OH)_4Ca_{0.54}Mg_{0.02}$.

Isothermal and dynamic gravimetry experiments were performed with a thermobalance produced by Netzsch GmbH, West Germany. Isothermal weight loss was followed by immersing the solid, preheated at 473 K for 1 h, in a furnace pre-adjusted to 630, 670, 690, 710 and 730 K. This covers the range of dehydroxylation of the investigated nontronite. Non-isothermal thermogravimetry was carried out at a heating rate of 5 deg min^{-1} from ambient up to 1073 K.

Results and discussions

Isothermal gravimetry

Figure 1 illustrates the isothermal weight-change recordings of nontronite at 630–730 K, plotted as the percentage of the material dehydroxylated (α) as a function of time (t) in minutes. Analysis of the kinetic curves was performed by correlating the fraction α *vs* t, and using the nine currently employed solid-state reaction functions [12, 13]. This was done by employing the least squares straight line fit, and evaluating the correlation coefficient (r) and standard error of estimate (Se) in every case. The respective Arrhenius linear plots of $\log k$ *vs.* $1/T$ were tested similarly. Table 1 lists the data obtained. Table 1 reveals that, in general, linearization of the data for every mechanism is better for the lower temperatures; the straight line fit becomes poorer for the data relating to the higher temperatures. The isothermal dehydroxylation of nontronite in the tested temperature range seems to be reasonably described by both diffusion-controlled mechanism D_3 and D_4. This is clear from the low dispersion of the data ($Se = 7.7 \times 10^{-3}$) and the reasonably satisfactory relative linearity ($-\bar{r} = 0.975213$) covering the whole range of the decomposition curves. The mean activation energy associated with the dehydroxylation is 125 kJ·mol^{-1}.

Dynamic thermogravimetry

Figure 2 illustrates the dynamic weight-loss curve of Sampor nontronite, plotted as the fraction dehydroxylated (α) as a function of linearly increasing temperature

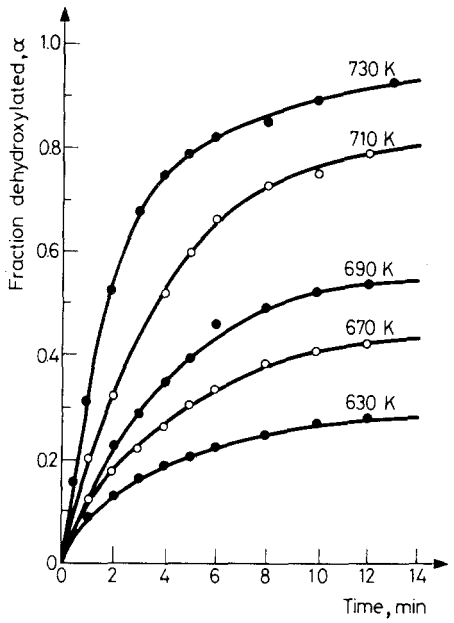

Fig. 1 Isothermal dehydroxylation of Sampor nontronite in the range of 630–730 K

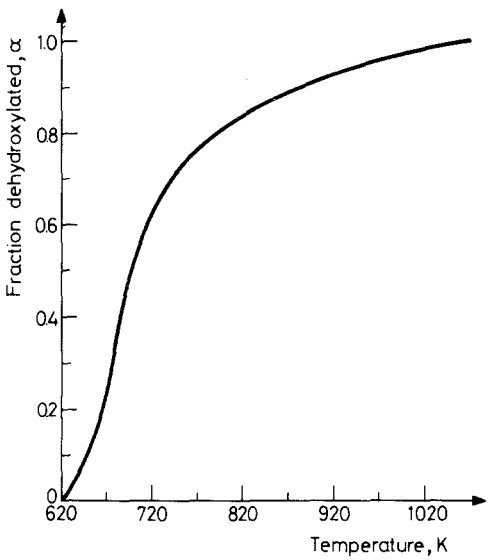

Fig. 2 Dynamic thermogravimetry of Sampor nontronite

Table 1 Kinetic parameters derived from isothermal dehydroxylation of nontronite

T, K	Parameter	D_1	D_2	D_3	D_4	F_1	A_2	A_3	R_2	R_3
	ln k	−5.1402	−5.7183	−7.1042	−7.1826	−3.9147	−3.7453	−3.8356	−4.7125	−5.0822
630	$-r$	0.973979	0.978377	0.981862	0.979666	0.936245	0.872582	0.857360	0.921908	0.925932
	Se × 10^3	7.4	3.32	0.77	0.76	38.1	64.2	63.6	18.3	12.3
	ln k	−4.3574	−4.8609	−6.1594	−6.2886	−3.4314	−3.6102	−4.2417	−4.8367	
670	$-r$	0.942879	0.944552	0.959790	0.957709	0.933195	0.904844	0.903169	0.923606	0.930437
	Se × 10^3	24.5	12.9	2.98	2.69	63.1	73.4	61.9	28.8	15.1
	ln k	−3.7718	−4.2256	−5.4691	−5.6624	−2.9535	−3.2421	−3.3274	−3.9069	−4.2349
690	−r	0.964167	0.971097	0.978293	0.954691	0.946172	0.912320	0.941705	0.906760	0.912205
	Se × 10^3	28.2	14.3	3.56	4.32	71.1	87.3	51.1	37.3	25.9
	ln k	−3.1895	−3.4097	−4.3621	−4.7308	−2.3073	−2.8941	−3.2759	−3.4914	−3.7383
710	−r	0.946186	0.967409	0.987668	0.975495	0.963089	0.934847	0.886480	0.924728	0.938629
	Se × 10^3	75.6	43.1	10.1	15.4	138.7	104.9	98.4	62.5	43.6
	ln k	−2.9158	−3.0075	−3.7108	−4.2486	−1.6812	−2.5945	−3.0108	−3.2047	−3.3809
730	$-r$	0.897479	0.940546	0.987109	0.960160	0.933501	0.893958	0.858887	0.889992	0.918063
	Se × 10^3	129.0	80.4	17.9	18.7	322.1	168.6	132.7	93.6	66.0
	$-\bar{r}$	0.904938	0.960422	0.978984	0.971442	0.942440	0.903778	0.889520	0.913398	0.925053
Mean	Se × 10^3	52.9	39.4	7.06	8.37	126.6	99.7	81.5	54.1	32.6
	E_a	89.2	107.9	133.1	116.0	84.9	43.8	31.1	62.0	68.5
Arrhenius	$-r$	0.993164	0.988049	0.978768	0.984773	0.967049	0.972714	0.977891	0.983503	0.956021
	Se × 10^3	12.1	19.5	32.2	23.7	25.8	12.1	7.6	8.2	24.1

(T, K). Analysis of the TG curve was carried out by correlating either log g(α) or log [g(α)/T^2] with $1/T$, as suggested by Šatava and Skvara (SS) [14], and the modified method of Coats and Redfern(CR) [15–17]. The tabulated data for log g(α) supplied by Šatava and Skvara for the nine commonly accepted solid-state reactions were used.

A linear regression analysis combined with a least squares straight line fit was used to test the best linearizing equation. The data obtained for optimization throughout the range $\alpha = 0.05$–0.95 are given in Table 2.

Table 2 Activation energy derived from the nonisothermal wave of dehydroxylation

Function	(SS)			(CR)		
	E_a, kJ·mol^{-1}	$-r$	Se × 10^2	E_a, kJ·mol^{-1}	$-r$	Se × 10^2
D_1	88.5	0.814370	43.1	64.9	0.743860	43.5
D_2	87.6	0.830467	26.7	83.5	0.867227	35.7
D_3	111.9	0.859518	44.6	88.0	0.825240	44.9
D_4	100.7	0.820488	42.5	79.4	0.799358	44.5
F_1	67.7	0.882119	22.8	54.2	0.812680	23.6
A_2	38.0	0.888614	11.1	27.2	0.850321	8.7
A_3	18.9	0.874579	7.8	10.3	0.822359	12.9
R_2	60.3	0.900676	20.2	37.2	0.826895	18.9
R_3	60.5	0.910589	22.2	47.3	0.778049	22.7
015	82.0	0.926135	21.6	58.5	0.891105	22.2
SO	98.1	0.951923	20.9	73.3	0.933359	21.3

These data indicate that each of the nine tested mechanisms resulted in a poor fit to the dynamic thermogravimetry of montronite. Very unsatisfactory, low values of the correlation coefficients ($-r = 0.820488$–0.910359 by SS, and $-r = 0.743860$–0.850321 by CR procedures) and a high dispersion of the data were observed. Two additional reaction mechanisms recommended by some authors [11, 18] were tried: second-order (SO) and one and one-half-order (015) mechanisms. The linearity of the straight line improved, but it still remained far from the satisfactory fit exhibited by a value approaching unity.

A further trial was made, in which the applied range of α was reduced in order to get better linearization. This was done on selected equations representing the D_2, D_3, R_2, F_1 and SO mechanisms, using four different decomposition ranges ($\alpha = 0.10$–$0.85, 0.10$–$0.75, 0.10$–0.65 and 0.10–0.55). The data obtained are given in Table 3. They reveal a successive improvement in the straight line fit, as evident from the progressive increase in r and the decrease in Se as functions of the decrease in the applied α range. This finding is valid for all the tested mechanism, but the activation energies increase in value. For the shortest limited range of decom-

Table 3 Change of activation energy and linear regression parameters on decreasing the range of fraction dehydroxylation (α)

Mechanism	Range of (α)	E_a, kJ·mol^{-1}	$-r$	Se × 10^3
	0.05–0.95	67.7	0.882119	22.8
	0.10–0.85	79.3	0.905010	15.1
F_1	0.10–0.75	105.2	0.953761	9.78
	0.10–0.65	132.0	0.982108	5.61
	0.10–0.55	150.9	0.993745	3.03
	0.05–0.95	98.1	0.951923	20.9
	0.10–0.85	109.3	0.946306	12.9
SO	0.10–0.75	133.9	0.973579	10.2
	0.10–0.65	160.6	0.991354	4.79
	0.10–0.55	177.3	0.997871	2.08
	0.05–0.95	60.3	0.900676	20.2
	0.10–0.85	69.5	0.901677	13.2
R_2	0.10–0.75	92.9	0.939388	9.9
	0.10–0.65	101.1	0.974512	6.0
	0.10–0.55	138.9	0.989259	3.6
	0.05–0.95	87.6	0.830457	26.7
	0.10–0.85	123.1	0.898253	24.8
D_2	0.10–0.715	168.5	0.935027	19.6
	0.10–0.65	220.9	0.970693	12.5
	0.10–0.55	260.1	0.990369	6.69
	0.05–0.95	111.9	0.859518	44.6
	0.10–0.85	136.8	0.909921	26.7
D_3	0.10–0.75	184.1	0.945011	21.1
	0.10–0.65	236.9	0.977037	11.6
	0.10–0.55	275.5	0.992103	6.4

position (α = 0.10–0.55, the F_1 and *SO* mechanisms seem to show the best straight line fit (cf. Table 3). The corresponding estimated activation energies are 151 and 177 kJ·mol^{-1}, respectively. Since a second-order solid-state decomposition mechanism is usually insignificant, the activation energy of 151 kJ·mol^{-1} would more reasonably represent the energy associated with the dehydroxylation of nontronite under the non-isothermal conditions. This value is ~20% higher than that estimated from the isothermal weight-change curves, as stated above. A diffusion-controlled mechanism seems to govern the isothermal curves recorded after the sudden increase in temperature. However, a first-order unimolecular dehydroxylation mechanism (F_1) seems to hold up to 60% decomposition in the gradual heating.

A plot had previously been proposed by Sharp et al. [12] for determination of the prevailing solid-state decomposition mechanism. This was applied here by plotting α *vs.* $t/t_{0.5}$ for the thermoanalytical curves ($t_{0.5}$ is the time elapsed to 50% reaction: $t = \left(\frac{T\,°C}{\beta(\text{deg/min})}\right)$. Figure 3 illustrates the reduced time scale plots of both the

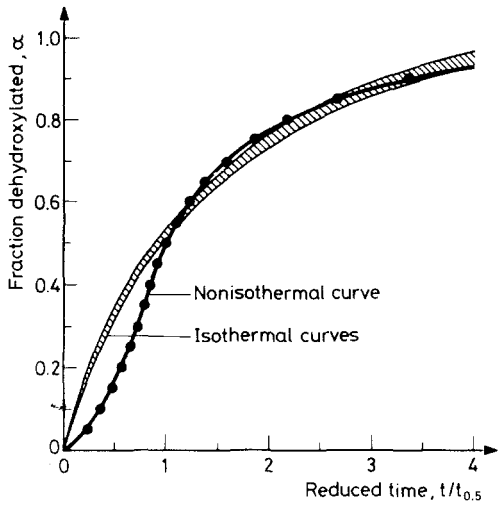

Fig. 3 Reduced time curves of isothermal and non-isothermal gravimetry

isothermal and non-isothermal gravimetry of nontronite superimposed on each other. Both series of analyses fall on an approximated curve at $\alpha \geqslant 0.5$, but the dynamic curve falls below the isothermal one at $\alpha \leqslant 0.5$. The reduced time isothermal curve (Fig. 3) corresponds to a mixed-type mechanism. In the early stages it is diffusion-controlled, and becomes a first-order one in the later stages of dehydroxylation. This conforms well with the data in Table 1. The reduced time plot of the dynamic curve also indicates a mixed-type mechanism (A_2 and F_1). This proves that no simple decomposition mechanism can adequately describe the dehydroxylation of the dioctahedral nontronite.

Finally, a comparison could be made with an American specimen of nontronite, investigated earlier [19].

The isothermal weight-change experiments gave exactly the same rate-controlling mechanism (D_3 and D_4) and the same activation energy, 122 ± 3 kJ·mol^{-1}. The non-isothermal curves reveal the same poor applicability to the currently accepted kinetic solid-state reaction mechanisms. A second-order equation seems to apply in both cases and yields almost the same activation energy (in the same α range): 135 ± 5 kJ·mol^{-1}.

References

1 N. H. Brett, K. J. D. Mackenzie and J. H. Sharp, Quart. Rev., 24 (1970) 1985.
2 I. Horvath and L. Galikova, Chem. Zvesti, 33 (1979) 604.
3 H. S. Robertson, Mineral. Polon., 11 (1980) 3.
4 H. M. Koster, Develop. Sediment. 35, International Clay Conference 1981, p. 41.
5 G. Margomenou Leonidopoulou and M. Laskou, Thermal Anal., Proc. Int. Conf. 7th, 1981, p. 551.
6 I. Novak and L. Novakova, Chem. Zvesti, 34 (1980) 348.
7 A. Alietti and M. F. Brigatti, Miner. Petrogr. Acta, 26 (1982) 39.
8 I. Horvath, E. S. San'ko, E. A. Paukshtis and E. N. Yurchenko, Chem. Zvesti, 36 (1982) 515.
9 J. S. Venugopal, E. V. Hirannaiah and S. K. Majumder, J. Geol. Soc. India, 23 (1982) 300.
10 J. Schomburg, Z. Geol. Wiss. Berlin, 12 (1984) 457.
11 I. Horvath, 5th Meeting of the European Clay Groups, Prague, 1983, 77.
12 J. H. Sharp, G. W. Brindley and B. N. N. Achar, J. Am. Ceram. Soc., 49 (1966) 379.
13 H. Tanaka, S. Shimada and H. Negita, Int. J. Chem. Kin., 17 (1985) 149.
14 V. Šatava and F. Skvara, J. Am. Ceram. Soc., 52 (1969) 591.
15 A. W. Coats and J. P. Redfern, Nature (London) 201 (1964) 68.
16 J. P. Elder, in "Analytical Calorimetry", Ed. J. F. Johnson and P. S. Gill, Plenum Corp. 1984, p. 255.
17 H. Tanaka and M. Tokumitsu, J. Thermal Anal., 29 (1984) 87.
18 Z. Adonyi and G. Kőrősi, Thermochim. Acta, 60 (1983) 23.
19 B. S. Girgis and N. S. Felix, J. Thermal Anal., 32 (1987) 1867.

Zusammenfassung — Mittels der Titeltechniken wurde im Bereich 570–1070 K ein reines typisches Nontronit aus der ČSSR (Sampor) untersucht. Die isotherme Dehydroxylierung von Nontronit bei 630–730 K konnte im Bereich der Zersetzung von $\alpha = 0{,}05$–$0{,}95$ durch die diffusionsbestimmten Mechanismen D_3 und D_4 befriedigend beschrieben werden. Eine Anwendung der Gleichungen für Feststoffreaktionen auf die nichtisotherme Kurve ergab mit Ausnahme des Bereiches $\alpha = 0{,}10$–$0{,}55$ nur sehr unzureichende Ergebnisse. Eine Gleichung für einen monomolekularen (F_1) Mechanismus sowie für einen mechanismus zweiter ordnung (SO) ergaben die beste Linearisierung der Kurve. Die aufgrund der isothermen (D_3, D_4) und nichtisothermen (F_1) Experimente geschätzten Aktivierungsenergien betragen 125 bzw. 151 kJ·mol^{-1}. Es wird angenommen, daß es sich bei beiden Techniken um eine Sequenz verschiedener Mechanismen handelt.

Резюме — Методом изотермической и неизотермической гравиметрии изучен в температурном интервале 570–1070 К чистый типичный нонтронит месторождения Шампор (Чехословакия). Изотермическое дегидроксилирование, проведенное в интервале температур 630–730 К со степенью превращения $\alpha = 0{,}05$–$0{,}95$, хорошо описывается диффузионно-контролирующими механизмами D_3 и D_4. Применение к неизотермической кривой уравнений несущих твердотельных реакций привело к плохим результатам, за исключением узкой области разложения с $\alpha = 0{,}10$–$0{,}55$. Применение одномолекулярного механизма реакции (F_1), а также механизма реакции второго порядка дало наилучшую линеаризацию кривой. Энергии активации, установленные на основе изотермических (D_3, D_4) и неизотермических (F_1) измерений, разнялись, соответственно, 125 и 151 кдж·моль$^{-1}$. Приведенные временные графики показали возможное наличие последовательности различных механизмов для обоих методов.